Cell Reports Medicine, Volume *2*

Supplemental Information

Targeted brachyury degradation disrupts a highly specific autoregulatory program controlling chordoma cell identity

Hadley E. Sheppard, Alessandra Dall'Agnese, Woojun D. Park, M. Hamza Shamim, Julien Dubrulle, Hannah L. Johnson, Fabio Stossi, Patricia Cogswell, Josh Sommer, Joan Levy, Tanaz Sharifnia, Mathias J. Wawer, Behnam Nabet, Nathanael S. Gray, Paul A. Clemons, Stuart L. Schreiber, Paul Workman, Richard A. Young, and Charles Y. Lin

Supplemental information

Figure S1: Brachyury is a master transcriptional regulator that defines the chordoma super enhancer landscape. Related to Figure 1.

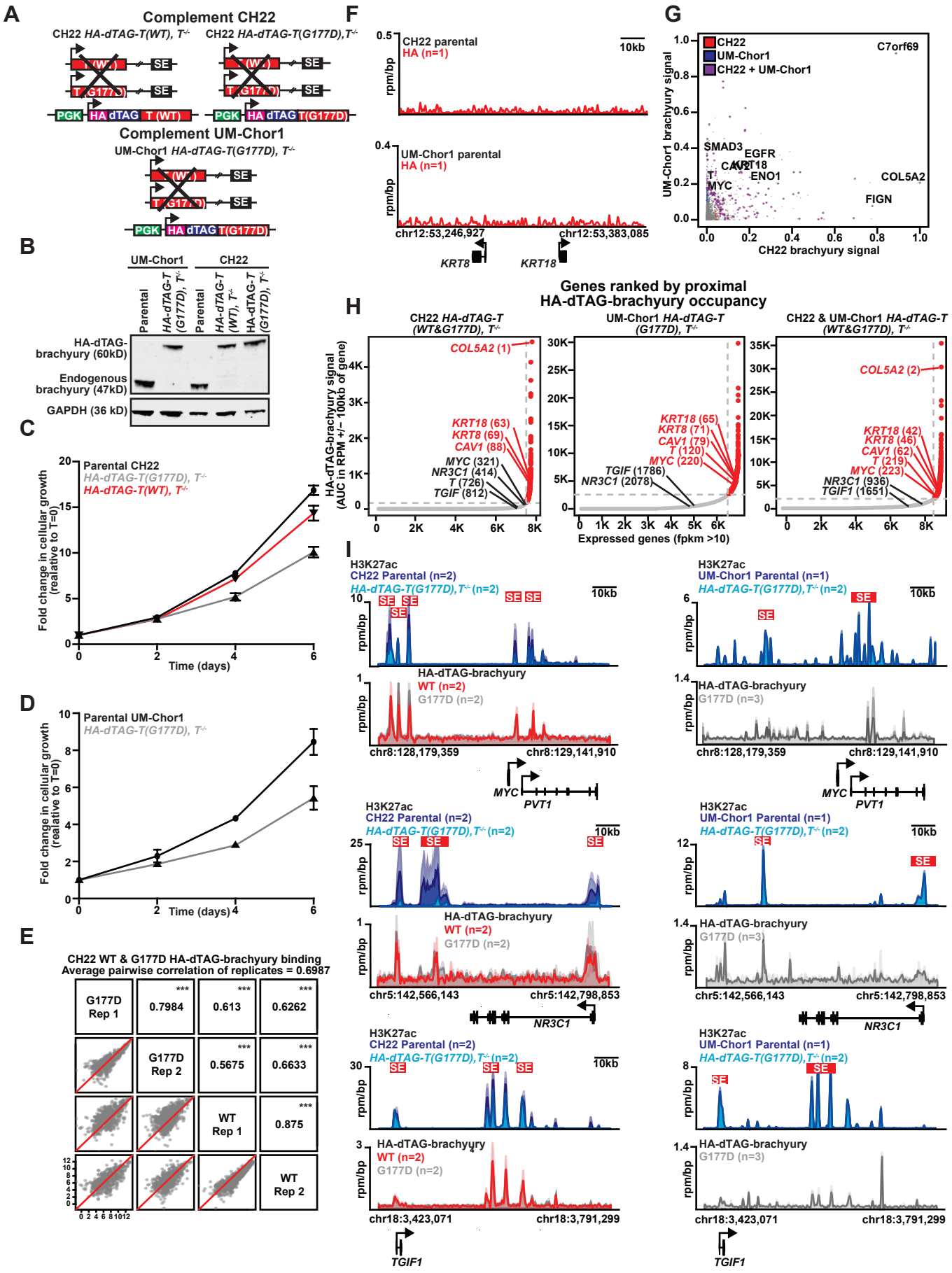

Figure S1: Brachyury is a master transcriptional regulator that defines the chordoma super enhancer landscape. Related to Figure 1.

A) Schematic depicting engineered chordoma cell lines (UM-Chor1 and CH22).

B) Immunoblot depicting brachyury levels in CH22 *HA-dTAG-T(WT), $T^{-/-}$*, CH22 *HA-dTAG-T(G177D), $T^{-/-}$* and UM-Chor1 *HA-dTAG-T(G177D), $T^{-/-}$* engineered chordoma cell lines. Cell lysates were subjected to immunoblots with a brachyury antibody. The shift in molecular weight is of the size expected for the HA-dTAG-brachyury fusion.

C) Fold change (relative to *t*=0) cell growth of CH22 parental, *HA-dTAG-T(WT), $T^{-/-}$* or *HA-dTAG-T(G177D), $T^{-/-}$* chordoma cells (n=3 biological replicates).

D) Fold change (relative to *t*=0) cell growth of UM-Chor1 parental or *HA-dTAG-T(G177D), $T^{-/-}$* chordoma cells (n=3 biological replicates).

E) Scatter plots of brachyury peak AUC between brachyury WT and brachyury G177D ChIPmentation biological replicates (n=2 WT, n=2 G177D). Pearson correlations are noted, indicating the high similarity between WT and G177D brachyury.

F) Gene tracks of HA peaks in CH22 and UM-Chor1 parental cell lines (units of reads per million per base pair) at the *KRT8/KRT18* loci (n=1 biological replicate each).

G) Scatter plot depicting expressed brachyury-regulated genes (identified by proximal brachyury signal) in UM-Chor1 *HA-dTAG-T(G177D), $T^{-/-}$,* versus CH22 *HA-dTAG-T(WT&G177D), $T^{-/-}$,* chordoma cells. The red genes are those only expressed in CH22 *HA-dTAG-T(WT&G177D),* the blue genes are those only expressed in UM-Chor1 *HA-dTAG-T(G177D), $T^{-/-}$,* and the purple genes are shared between the two cell lines. For CH22, n=4 biological replicates For UM-Chor1, n=3 biological replicates.

H) Enhancers in the chordoma cell lines CH22 *HA-dTAG-T(WT&G177D), $T^{-/-}$,* UM-Chor1 *HA-dTAG-T(G177D), $T^{-/-}$* and the combination all three cell lines ranked by average brachyury signal. SEs are denoted in red and associated genes are annotated. For CH22, n=4 biological replicates For UM-Chor1, n=3 biological replicates.

I) Gene tracks of H3K27ac and HA (HA-dTAG-brachyury) (units of reads per million per base pair at the *MYC, NR3C1 and TGIF* loci in CH22 or UM-Chor1 parental and *HA-dTAG-T, $T^{-/-}$* chordoma cells. SEs are denoted by red boxes. For CH22, n=4 biological replicates for H3K27ac and HA-dTAG-brachyury, respectively. For UM-Chor1, n=3 biological replicates for H3K27ac and HA-dTAG-brachyury, respectively.

Figure S2: Brachyury autoregulates through a super enhancer transcriptional condensate. Related to Figure 2.

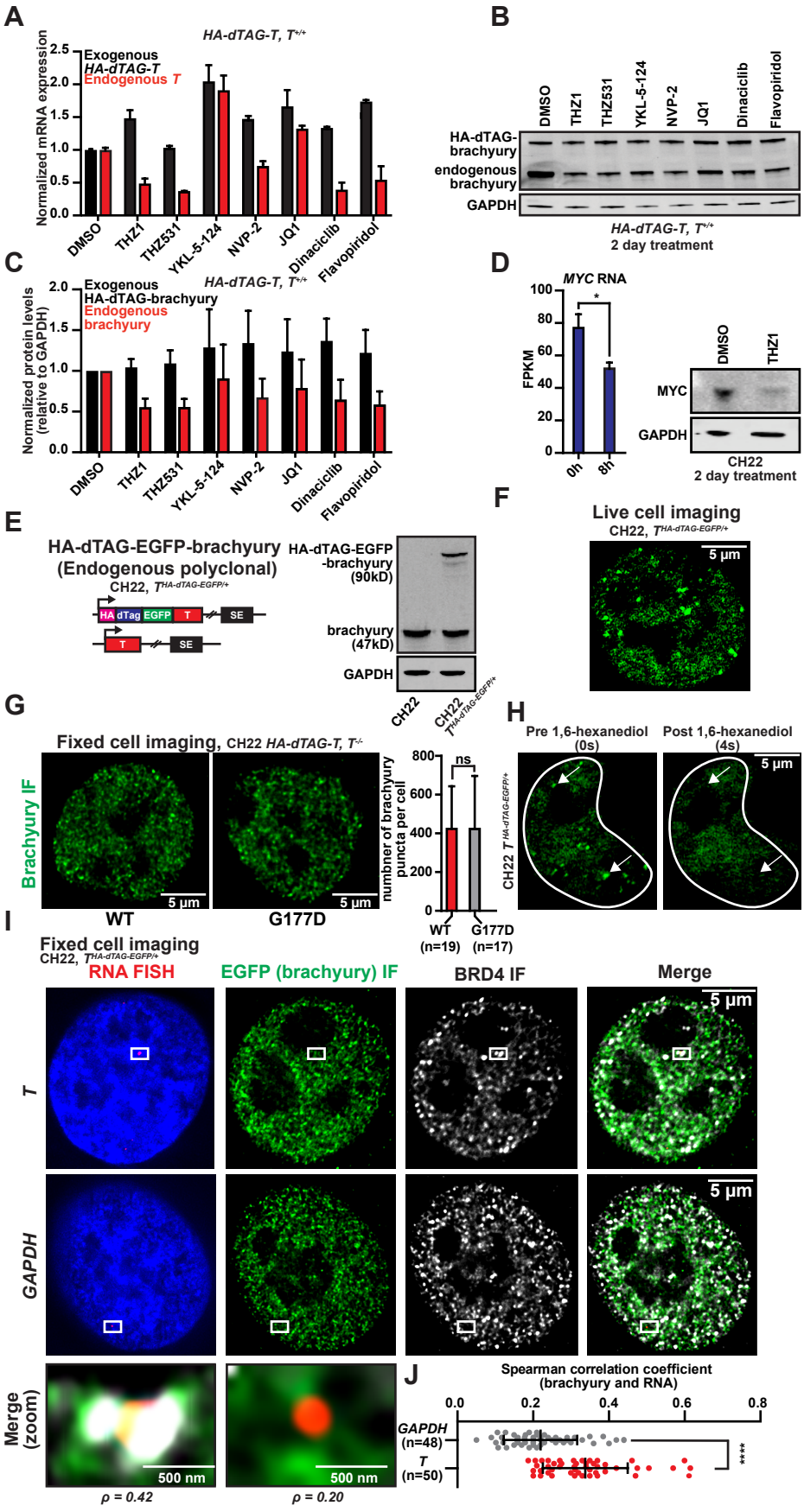

Figure S2: Brachyury autoregulates through a super enhancer transcriptional condensate. Related to Figure 2.

A) Bar plot depicting mRNA levels by qPCR of exogenous *HA-dTAG-T* and endogenous *T* in *HA-dTAG-T,T*$^{+/+}$ CH22 chordoma cells treated with the indicated compounds or DMSO for 8 hours. N=3 technical replicates and error bars denote +/- s.d. Concentrations of the compounds are as follows: THZ1 60nM, THZ531 100nM, YKL-5-124 1μM, NVP-2 60nM, JQ1 3μM, dinaciclib 50nM, flavopiridol 350nM.

B) Representative immunoblot depicting protein levels of exogenous HA-dTAG-brachyury and endogenous brachyury in *HA-dTAG-T,* $T^{+/+}$ CH22 chordoma cells treated with the indicated compounds or DMSO for 2 days. Concentrations of the compounds are as follows: THZ1 60nM, THZ531 100nM, YKL-5-124 1μM, NVP-2 60nM, JQ1 3μM, dinaciclib 50nM, flavopiridol 350nM.

C) Quantification of protein levels (n=2 biological replicates) from immunoblot in S2B and a second biological replicate. Error bars denote +/- s.d.

D) *MYC* mRNA (n=3 biological replicates per treatment) and MYC protein levels (1 biological replicate) in CH22 chordoma cells treated with 60nM THZ1 at the indicated time point. For mRNA levels, error bars denote +/- SEM. For protein levels, error bars denote +/- s.d.

E) Left: Schematic depicting engineered cell line chordoma, CH22, $T^{HA\text{-}dTAG\text{-}EGFP/+}$. Right: Immunoblot of endogenous expression levels of HA-dTAG-EGFP-brachyury in either polyclonal CH22, $T^{HA\text{-}dTAG\text{-}EGFP/+}$ or parental CH22 chordoma cells.

F) Live imaging of CH22, $T^{HA\text{-}dTAG\text{-}EGFP/+}$ chordoma cells showing discrete brachyury puncta.

G) Left: Fixed-cell IF of brachyury in CH22 *HA-dTAG-T(WT),* $T^{-/-}$ and CH22 *HA-dTAG-T(G177D),* $T^{-/-}$ chordoma cells. Right: Quantification of the number of brachyury puncta in CH22 *HA-dTAG-T(WT),* $T^{-/-}$ and CH22 *HA-dTAG-T(G177D),* $T^{-/-}$ chordoma cells, respectively. This experiment was performed with one biological replicate, each.

H) Representative images of CH22, $T^{HA\text{-}dTAG\text{-}EGFP/+}$ chordoma cells before and after treatment with 3% hexanediol for 4s (n=1 biological replicate).

I) Top: Colocalization between BRD4 and *T* nascent RNA by IF and nascent RNA FISH, respectively, in fixed CH22, $T^{HA\text{-}dTAG\text{-}EGFP/+}$ chordoma cells. Bottom: Colocalization between BRD4 and *GAPDH* nascent RNA by IF and nascent RNA FISH in fixed CH22, $T^{HA\text{-}dTAG\text{-}EGFP/+}$ chordoma cells. Separate images of the indicated IF and FISH are shown, along with a merged image. The rightmost column shows the area in the white box in greater detail, along with the calculated spearman correlation coefficient for BRD4 protein and *T* or *GAPDH* nascent RNA colocalization.

J) Quantification of *T* nascent RNA and brachyury protein colocalization compared to *GAPDH* nascent RNA and brachyury protein colocalization (cells from two biological populations were prepared and imaged in parallel). Spearman correlation coefficients between either *T* or *GAPDH* nascent RNA and with brachyury protein signal are plotted. ****P<0.0001, derived from a two-tailed, unpaired *t* test.

Figure S3: Transcriptional CDK inhibition-induced apoptosis is associated with brachyury downregulation. Related to Figure 3.

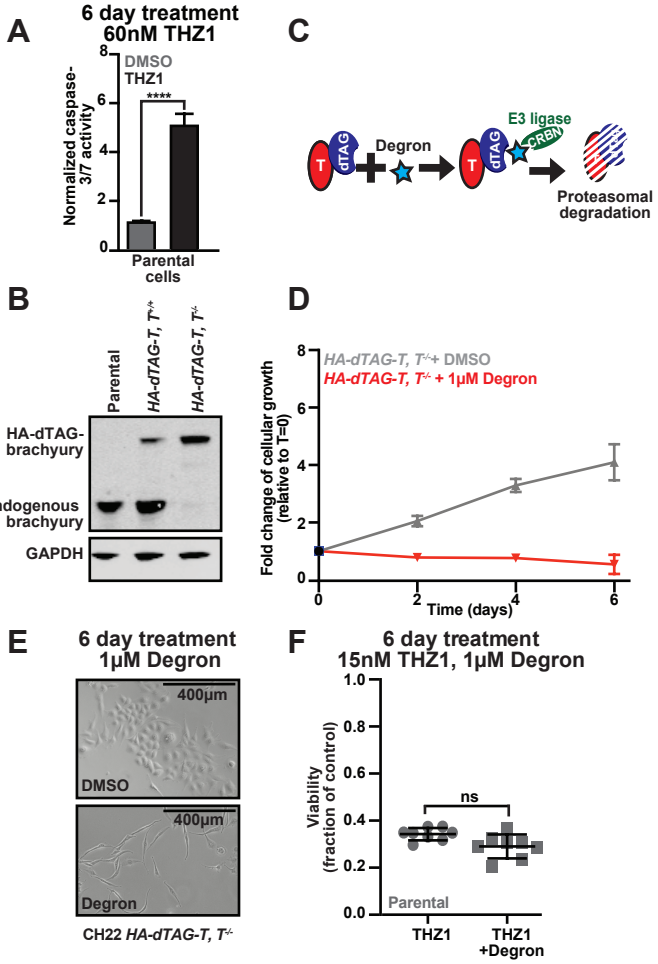

Figure S3: Transcriptional CDK inhibition-induced apoptosis is associated with brachyury downregulation. Related to Figure 3.

A) Caspase-3/7 levels following THZ1 treatment of CH22 chordoma cells. Caspase-3/7 levels and cell viability were measured in parallel. Data are plotted as the normalized mean level of caspase-3/7 to DMSO-treated cells, normalized again to the cell viability for each treatment (n=5 biological replicates). Error bars denote ± s.d. ****P<0.0001, derived from a two-tailed, unpaired *t* test.

B) Immunoblot showing brachyury levels in *HA-dTAG-T,* $T^{+/+}$ polyclonal CH22 chordoma cells and *HA-dTAG-T,* $T^{-/-}$ clonal CH22 chordoma cells.

C) Schematic depicting dTAG mechanism for targeted brachyury degradation. In brief, the N-terminus of transgenic brachyury is tagged with the dTAG. When exposed to a small molecule (degron), dTAG-brachyury is ubiquitylated and rapidly degraded.

D) Fold change (relative to *t*=0) cellular growth of *HA-dTAG-T,* $T^{-/-}$ CH22 chordoma cells treated with either DMSO or 1μM degron treatment (n=3 biological replicates). Error bars denote ± s.d.

E) Representative images of the morphological changes that occur with degron treatment in *HA-dTAG-T,* $T^{-/-}$ CH22 chordoma cells.

F) Cell viability of CH22 parental chordoma cells treated with 15nM THZ1 or 1 μM degron + 15nM THZ1 for 6 days. Data are plotted as the mean of the fraction of cell viability relative to DMSO-treated cells (n=8 biological replicates). Error bars denote ± s.d.

Figure S4: Brachyury is a highly selective transcriptional regulator. Related to Figure 4.

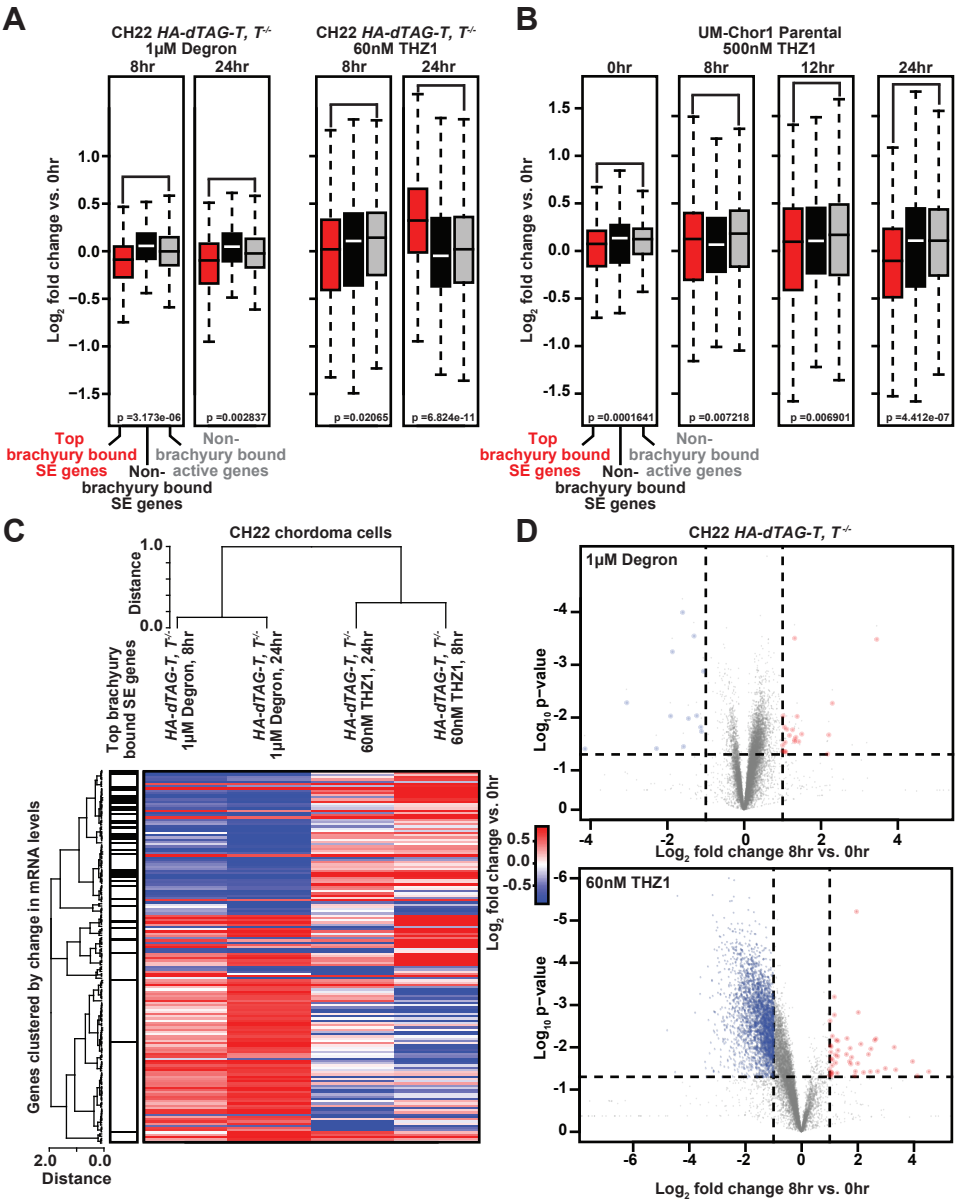

Figure S4: Brachyury is a highly selective transcriptional regulator. Related to Figure 4.

A) Boxplots depicting the log_2 fold change in total mRNA with degron or THZ1 treatment in CH22 *HA-dTAG-T, $T^{-/-}$* chordoma cells (n=3 biological replicates per treatment). Red boxes denote the top brachyury-bound SE-associated genes, black boxes denote non-brachyury-bound SE-associated genes, and gray boxes denote non-brachyury-bound active genes.

B) Boxplots showing the log_2 fold change in total mRNA with THZ1 treatment in parental UM-Chor1 chordoma cells (n=3 biological replicates per treatment). Red boxes denote the top brachyury-bound SE-associated genes, black boxes denote non-brachyury-bound SE-associated genes, and gray boxes denote non-brachyury-bound active genes.

C) Heatmap denoting the differential change in gene expression with THZ1 or degron treatment in CH22 *HA-dTAG-T, $T^{-/-}$* chordoma cells (n=3 biological replicates per treatment). The top brachyury-bound SE genes are indicated on the left.

D) Top: Volcano plot showing the log_2 fold change in total gene expression with 8-hour degron treatment in CH22 *HA-dTAG-T, $T^{-/-}$* chordoma cells (n=3 biological replicates per treatment). Blue dots indicate genes that exhibited a log_2 fold change less than -1 with a corresponding p-value less than 0.05. Red dots indicate genes that exhibited a log_2 fold change greater than 1 with a corresponding p-value less than 0.05. Bottom: Volcano plot showing the log_2 fold change in total gene expression with 8-hour THZ1 treatment in CH22 *HA-dTAG-T, $T^{-/-}$* chordoma cells (n=3 biological replicates per treatment). Blue dots indicate genes that exhibited a log_2 fold change less than -1 with a corresponding p-value less than 0.05. Red dots indicate genes that exhibited a log_2 fold change greater than 1 with a corresponding p-value less than 0.05.

Figure S5: THZ1 and brachyury degradation converge on disrupting the *T* transcriptional condensate. Related to Figure 5.

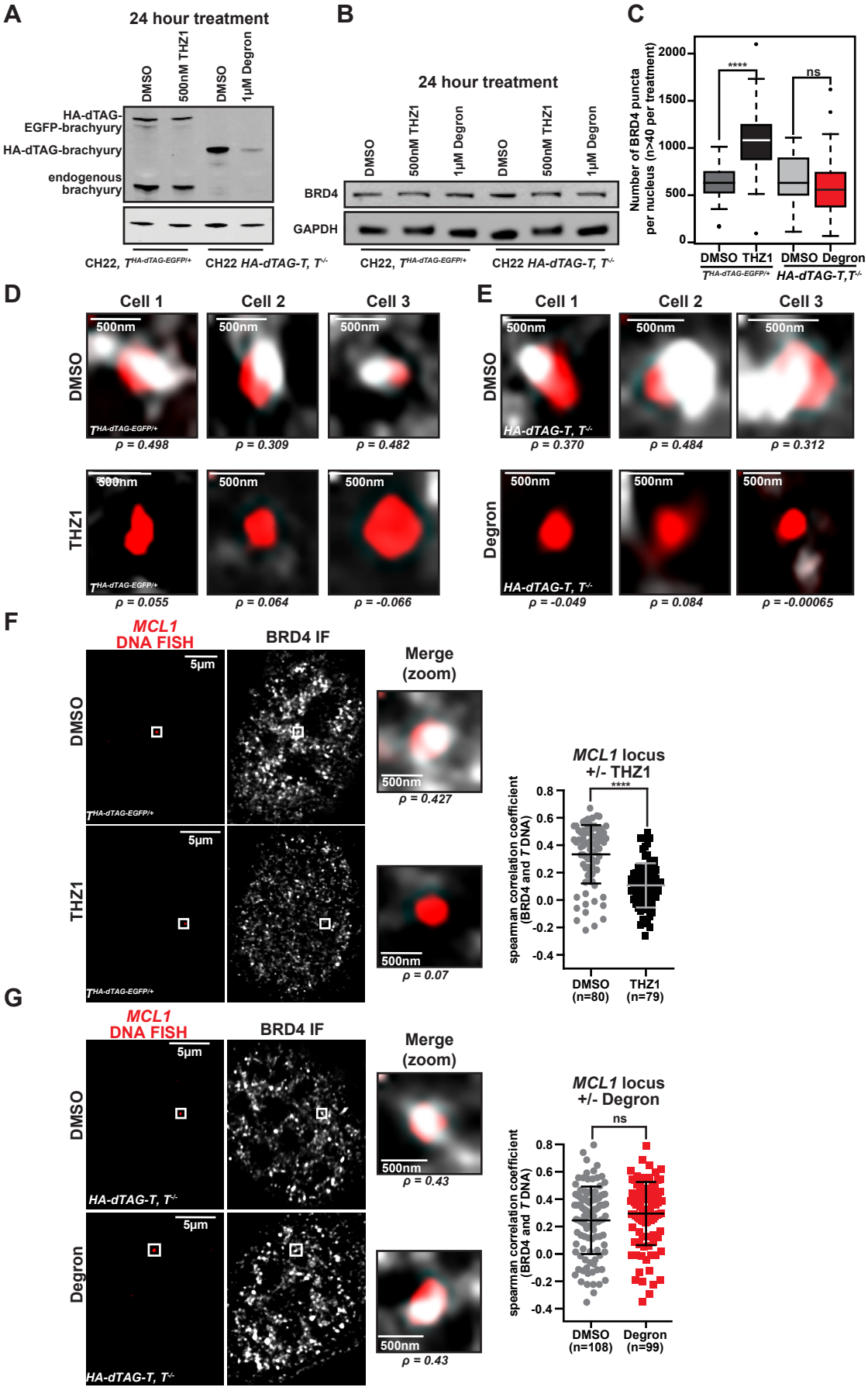

Figure S5: THZ1 and brachyury degradation converge on disrupting the *T* transcriptional condensate. Related to Figure 5.

A) Immunoblot depicting brachyury levels with 24-hour treatment of either 500nM THZ1 or 1μM degron in CH22, $T^{HA\text{-}dTAG\text{-}EGFP+}$ and CH22 *HA-dTAG-T,* $T^{-/-}$ chordoma cells, respectively.

B) Immunoblot of BRD4 levels in CH22, $T^{HA\text{-}dTAG\text{-}EGFP/+}$ cells or *HA-dTAG-T,* $T^{-/-}$ CH22 chordoma cells with DMSO, 500nM THZ1 or 1μM degron (n=1).

C) Quantification of the total number of BRD4 puncta in CH22, $T^{HA\text{-}dTAG\text{-}EGFP/+}$ chordoma cells or *HA-dTAG-T,* $T^{-/-}$ CH22 chordoma cells with either 500nM THZ1 or 1μM degron, respectively. ****P<0.0001, derived from a two tailed, unpaired *t* test (n=1).

D) Merged images showing colocalization of BRD4 protein (by IF) and the *T* DNA locus (by DNA FISH) in fixed CH22, $T^{HA\text{-}dTAG\text{-}EGFP/+}$ chordoma cells with 500nM THZ1 or DMSO. The spearman correlation coefficient for BRD4 protein and the *T* DNA locus signal is calculated for each image.

E) Merged images showing colocalization of BRD4 protein (by IF) and the *T* DNA locus (by DNA FISH) in CH22 *HA-dTAG-T,* $T^{-/-}$ chordoma cells with 1μM degron or DMSO. The spearman correlation coefficient for BRD4 protein and the *T* DNA locus signal is calculated for each image.

F) Left**:** Colocalization between BRD4 and the *MCL1* DNA locus by IF and DNA FISH, respectively, in fixed CH22, $T^{HA\text{-}dTAG\text{-}EGFP/+}$ chordoma cells with 500nM THZ1 or DMSO (24 hours). Right: Quantification of spearman correlation coefficients between *MCL1* DNA FISH signal and BRD4 protein with either 500nM THZ1 or DMSO. Three biological replicates were treated and imaged in parallel. ****P<0.0001, derived from a two tailed, unpaired *t* test.

G) Left: Colocalization between BRD4 and the *MCL1* DNA locus by IF and DNA FISH, respectively, in fixed CH22 *HA-dTAG-T,* $T^{-/-}$ chordoma cells with 1μM degron or DMSO (24 hours). Right: Quantification of spearman correlation coefficients between *T* DNA FISH signal and BRD4 protein signal with either 1μM Degron or DMSO. Three biological replicates were treated and imaged in parallel. P>0.05, derived from a two-tailed, unpaired *t* test.

Figure S6: Brachyury degradation induces senescence and sensitizes chordoma cells to anti-apoptotic inhibitors. Related to Figure 6.

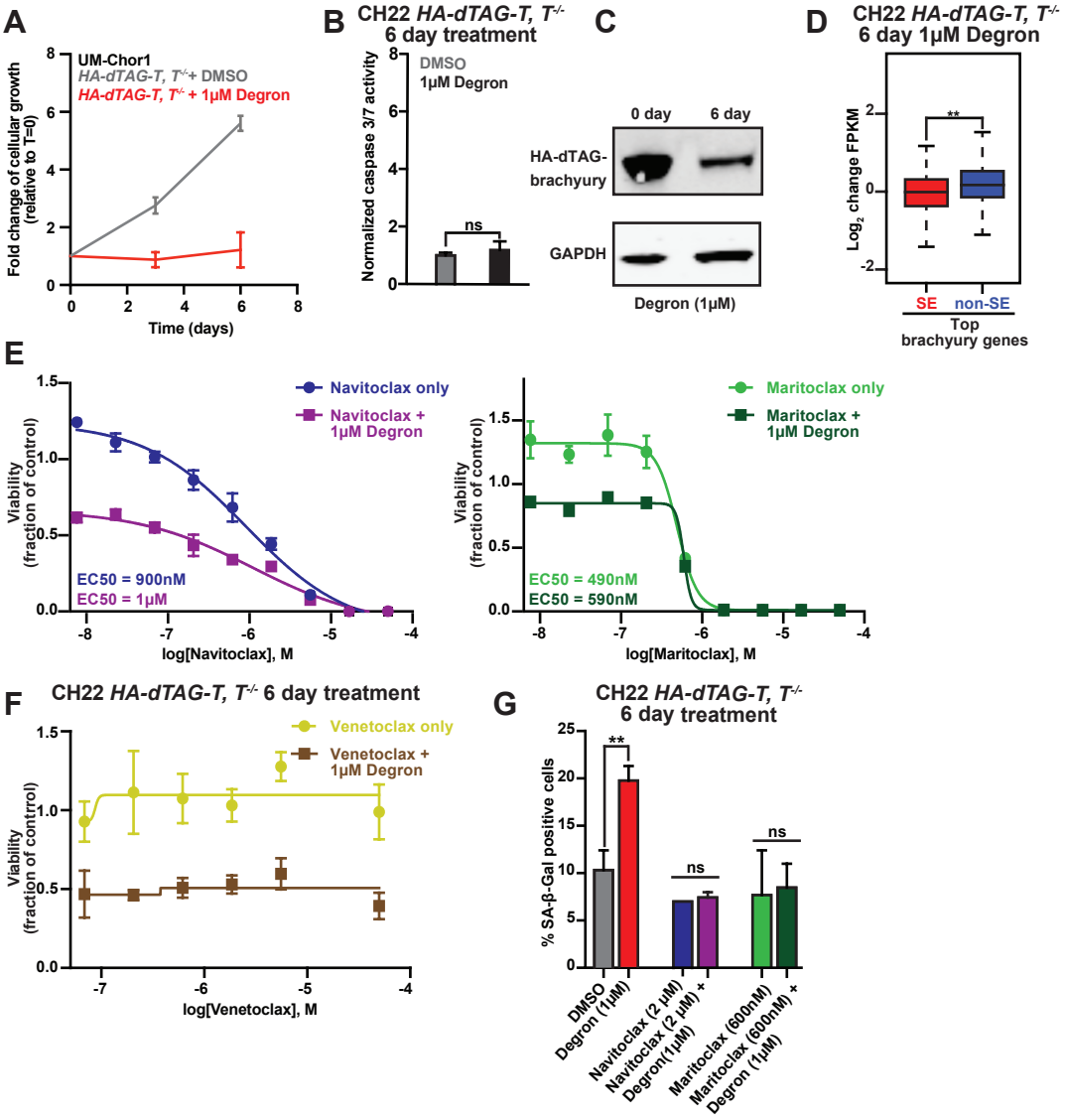

Figure S6: Brachyury degradation induces senescence and sensitizes chordoma cells to anti-apoptotic inhibitors. Related to Figure 6.

A) Fold change (relative to *t*=0) cellular growth of *HA-dTAG-T, T*$^{-/-}$ UM-Chor1 chordoma cells treated with either DMSO or 1μM degron treatment (n=3 biological replicates).

B) Caspase-3/7 levels in CH22 *HA-dTAG-T, T*$^{-/-}$ chordoma cells treated with 1 μM degron for 6 days. Caspase-3/7 levels and cell viability were measured in parallel. Data are plotted as the normalized mean level of caspase-3/7 activity relative to DMSO-treated cells, normalized again to the cell viability for each treatment. Error bars represent ± s.d. (n=3 biological replicates). P>0.05, derived from a two-tailed, unpaired *t* test.

C) Immunoblot validating brachyury degradation corresponding to S6D with 6-day degron treatment in CH22 *HA-dTAG-T, T*$^{-/-}$ chordoma cells (n=1).

D) Boxplot depicting the $\log_2$ change in FPKM of genes with 6-day degron treatment in CH22 *HA-dTAG-T, T*$^{-/-}$ chordoma cells (n=3 biological replicates per treatment). The red box denotes the top brachyury-bound, SE-associated genes and the blue box denotes the top brachyury-bound, non-SE-associated genes.

E) Validation of maritoclax and navitoclax sensitivity in CH22 *HA-dTAG-T, T*$^{-/-}$ chordoma cells +/- 1μM degron. Cells were treated with indicated concentrations of compound and assayed for cell viability after 6 days. The X axis indicates the log of drug concentration and the Y axis indicates response (cellular viability relative to DMSO-treated cells, n=3 biological replicates).

F) Validation of venetoclax sensitivity in CH22 *HA-dTAG-T, T*$^{-/-}$ chordoma cells +/- 1μM degron. Cells were treated with indicated concentrations of compound and assayed for cell viability after 6 days. The X axis indicates the log of drug concentration and the Y axis indicates response (cellular viability relative to DMSO-treated cells, n=3 biological replicates).

G) Percentage of SA-ß-gal positive CH22 *HA-dTAG-T, T*$^{-/-}$ chordoma cells treated with DMSO, 1μM degron alone, 600nM maritoclax alone, 2 μM navitoclax alone, or 1μM degron in combination with 600nM maritoclax or 2μM navitoclax for 6 days. Error bars denote ± s.d. (n=3 biological replicates). **P<0.01, derived from a two-tailed, unpaired *t* test.

Table S1: Top upregulated gene signatures with 24-hour degron treatment. Related to Figure 4.

Name	Normalized Enrichment Score	FDR q-value
REACTOME_AMYLOIDS	2.674376	0
KEGG_SYSTEMIC_LUPUS_ERYTHEMATOSUS	2.640108	0
DAZARD_UV_RESPONSE_CLUSTER_G2	2.639163	0
REACTOME_RNA_POL_I_PROMOTER_OPENING	2.585501	0
NAGASHIMA_EGF_SIGNALING_UP	2.5717456	0
NAGASHIMA_NRG1_SIGNALING_UP	2.552744	0
REACTOME_RNA_POL_I_TRANSCRIPTION	2.5021663	0
SMIRNOV_RESPONSE_TO_IR_2HR_UP	2.45989	0
ZWANG_CLASS_3_TRANSIENTLY_INDUCED_BY_EGF	2.4462447	0
BILD_HRAS_ONCOGENIC_SIGNATURE	2.4108276	0

Table S2: Top upregulated gene signatures with 24-hour THZ1 treatment. Related to Figure 4.

Name	Normalized Enrichment Score	FDR q-value
MARTENS_TRETINOIN_RESPONSE_UP	2.414513	0
HECKER_IFNB1_TARGETS	2.3230712	0
HAMAI_APOPTOSIS_VIA_TRAIL_DN	2.1642678	0.001063347
NIKOLSKY_BREAST_CANCER_16P13_AMPLICON	2.217807	0.001230881
SENGUPTA_NASOPHARYNGEAL_CARCINOMA_DN	2.1643865	0.001240572
MIKKELSEN_NPC_HCP_WITH_H3K27ME3	2.2030544	0.00129474
MIKKELSEN_IPS_LCP_WITH_H3K4ME3	2.172486	0.001488686
LIM_MAMMARY_LUMINAL_MATURE_UP	2.1566415	0.001490596
FARMER_BREAST_CANCER_CLUSTER_1	2.1401677	0.001737144
MOREAUX_B_LYMPHOCYTE_MATURATION_BY_TACI_UP	2.1200964	0.001858595

Table S3: HDR template for CRISPR-mediated endogenous tagging of the *T* gene. Related to STAR Methods.

Name	Sequence
HA-dTAG-EGFP-T	gctctatttatGGGGAGGGCACTGAATTTCGGTCCCCAGAGACCTACACTAGTAGA GCCTTGGGGAGTTCAAGTGGAATAACTTCTCCCCACCCCTCTGCCCCCGTCC CCTCCCCCCAAGTCTTGGTCCGCGCCCTCCTCCCGGGTCTGTGCCGGGACCC GGGACCCGGGAGCCGTCGCAGGTCTCGGTCCAAGGGGCCCCTTTTCTCGGA AGGGCGGCGGCCAAGAGCAGGGAAGGTGGATCTCAGGTAGCGAGTCTGGG CTTCGGGGACGGCGGGGAGGGGAGCCGGACGGGAGGATGatggtgagcaagggcga ggagctgttcaccggggtggtgcccatcctggtcgagctggacggcgacgtaaacggccacaagttcagcgtgtccggcga gggcgagggcgatgccacctacggcaagctgaccctgaagttcatctgcaccaccggcaagctgcccgtgccctggccca ccctcgtgaccaccctgacctacggcgtgcagtgcttcagccgctaccccgaccacatgaagcagcacgacttcttcaagtcc gccatgcccgaaggctacgtccaggagcgcaccatcttcttcaaggacgacggcaactacaagacccgcgccgaggtgaa gttcgagggcgacaccctggtgaaccgcatcgagctgaagggcatcgacttcaaggaggacggcaacatcctggggcaca agctggagtacaactacaacagccacaacgtctatatcatggccgacaagcagaagaacggcatcaaggtgaacttcaagat ccgccacaacatcgaggacggcagcgtgcagctcgccgaccactaccagcagaacaccccatcggcgacggccccgtg ctgctgcccgacaaccactacctgagcacccagtccgccctgagcaaagaccccaacgagaagcgcgatcacatggtcctg ctggagttcgtgaccgccgccgggatcactctcggcatggacgagctgtacaagggatctggatacccatacgatgttccag attacgctGCTAGCGGAGTGCAGGTGGAAACCATCTCCCCAGGAGACGGGCGCA CCTTCCCCAAGCGCGGCCAGACCTGCGTGGTGCACTACACCGGGATGCTTG AAGATGGAAAGAAAGTTGATTCCTCCCGGGACAGAAACAAGCCCTTTAAGT TTATGCTAGGCAAGCAGGAGGTGATCCGAGGCTGGGAAGAAGGGGTTGCCC AGATGAGTGTGGGTCAGAGAGCCAAACTGACTATATCTCCAGATTATGCCT ATGGTGCCACTGGGCACCCAGGCATCATCCCACCACATGCCACTCTCGTCTT CGATGTGGAGCTTCTAAAACTGGAAGGTGGCGGCAAATTCGGTGGCGGCAA ATTCAGCTCCCCTGGCACCGAGAGCGCGGGAAAGAGCCTGCAGTACCGAGT GGACCACCTGCTGAGCGCCGTGGAGAATGAGCTGCAGGCGGGCAGCGAGA AGGGCGACCCCACAGAGCGCGAACTGCGCGTGGGCCTGGAGGAGAGCGAG CTGTGGCTGCGCTTCAAGGAGCTCACCAATGAGATGATCGTGACCAAGAAC GGCAGgtgggtgcgcgtccggagcccgcgcgccgcgctctccagcgcctgggcagcctgggggacctggcaagt tcccggaggtcgaacccttttctcc